JOURNAL OF CATALYSIS **104**, 365–374 (1987)

# The Influence of Particle Size and Structure on the Mössbauer Spectra of Iron Carbides Formed during Fischer–Tropsch Synthesis

ROBERT R. GATTE AND JONATHAN PHILLIPS[1]

*Department of Chemical Engineering, The Pennsylvania State University, 133 Fenske Laboratory, University Park, Pennsylvania 16802*

Received July 15, 1986; revised November 3, 1986

A modeling routine which accounts for superparamagnetic relaxation, collective magnetic excitation, log–normal particle distribution, and quadrupole shift distribution was used to generate theoretical Mössbauer spectroscopic data, which were analyzed with a standard least-squares fitting routine. These spectra were used for comparison with published spectra of $\varepsilon$ and $\varepsilon'$ carbides. The results indicate that invariably, the Mössbauer spectra of small carbide particles exhibit relaxation effects, and proper analysis can only be achieved by collecting a series of spectra at different temperatures. In addition, a critical evaluation of the available Mössbauer parameters for $\varepsilon$ and $\varepsilon'$ carbides is presented along with equally feasible interpretations of these results.

## INTRODUCTION

The characterization of the bulk phase of iron catalyst particles which are active and stable during Fischer–Tropsch synthesis has been a matter of investigation for many years (*1–11*). Neither X-ray diffraction, Mössbauer spectroscopy, magnetic susceptibility, nor carbon content analysis has proven capable of unambiguously identifying the carbide phase(s) formed. It has been argued that as many as four distinct metastable carbide phases form during the Fischer–Tropsch reaction, which have relatively high carbon content (mole ratio C/Fe > 1/3). Similar phases have been identified as precipitates resulting from the tempering of martensite (*12–14*). (See Ref. (*12*) for an excellent review.) Two of these phases have been fully characterized. They are the Hägg, or $\chi$-carbide ($Fe_5C_2$), and cementite, or $\Theta$-carbide ($Fe_3C$). Both have been identified by X-ray diffraction, thermomagnetic studies, and Mössbauer spectroscopy (*8, 15–17*). In addition, perhaps two other metastable phases form during synthesis in which the iron atoms form a "nearly" hexagonally close-packed array, with the carbon atoms distributed in the octahedral holes (*9–11, 18*). These structures, which are usually present as very small crystallites (<10 nm), have been variously identified as $\varepsilon$-$Fe_2C$, as $\varepsilon'$-$Fe_{2.2}C$, or more generally as the octahedral carbides (*1*). It is the identity of these phases and the conditions of their formation which are least understood.

Extensive X-ray studies of iron-based Fischer–Tropsch catalysts have been conducted. Hofer *et al.* (*17*) presented a detailed investigation of $\chi$-carbide and cementite ($\Theta$-carbide). Barton and Gale (*18*) presented an analysis of what they believed to be $\varepsilon$-carbide, $Fe_2C$. In fact, most workers have tried to use X-ray diffraction to characterize their catalyst systems. However, the results have been unsatisfactory for a number of reasons. The carbided samples were generally commercial catalysts containing a number of additives (Si, Mn, Ni, Cr, etc.) (*8–10, 13–18*). The effect of the additives on the carbide structure and the X-ray data was not clarified. In addition, the particles were studied *ex situ*, following

---

[1] To whom correspondence should be addressed.

0021-9517/87 $3.00

air exposure, and were probably partially oxidized. Furthermore, the recent results (*1–7*) are from catalysts with relatively small crystallites (ca. 30–100 Å), so that very broad and in many cases poorly resolved lines were observed. Other workers have also discussed the unsuitability of these studies for yielding conclusive determinations of particle structure (*1*, *6*).

The use of Mössbauer spectroscopy for *in situ* studies of these catalysts has also led to conflicting reports. For instance, some investigators (*2–6*) have attempted to correlate the phase formed to the particle size, suggesting that $\chi$- and $\varepsilon'$-carbides coexist under reaction conditions and that $\varepsilon'$ is present only as small particles while $\chi$-carbide is the dominant phase in larger ones. Others (*8–10*) have argued that the dominant phases are $\varepsilon$ and $\varepsilon'$. Still others (*14*) have proposed that the presence of promoters, especially Si, stabilizes the $\varepsilon'$ phase allowing it to exist over a range of conditions. In addition LeCaër *et al.* (*1*) have presented arguments indicating that the identities of the $\varepsilon$-$Fe_2C$ and $\varepsilon'$-$Fe_{2.2}C$ phases are actually the reverse, $\varepsilon$-$Fe_{2.2}C$ and $\varepsilon'$-$Fe_2C$. Upon careful review of the available literature, it becomes clear that the problem lies in the analysis of the observed Mössbauer spectra.

It is evident that few reliable data regarding the Mössbauer parameters of bulk $\varepsilon$- or $\varepsilon'$-carbide exist. The parameters associated with $\varepsilon$-carbide have nearly always been obtained from spectra in which the carbide peaks are strongly overshadowed by those of iron oxide or $\alpha$-iron (*9*, *14*). Furthermore, the existence of the $\varepsilon'$ phase was first deduced simply on the basis of a discrepancy between the observed and theoretical population ratios of the peaks of hexagonal $\varepsilon$-carbide (*9*). Also, in those few studies where the strongest peaks *are* associated with an octahedral carbide phase (always $\varepsilon'$-carbide) (*2–7*), relaxed asymmetric spectra with broad peaks are produced. Yet, previous workers have usually fit these spectra with a single sextuplet. However, it has been argued (*1*) that there is no crystal structure that could support the $Fe_{2.2}C$ stoichiometry and possess a unique iron atom environment. This is necessary for the phase to exhibit a single sextuplet in the Mössbauer spectrum. None of these difficulties has been properly addressed in the available literature.

In the following, we present an investigation of the effects of relaxation on the observed Mössbauer spectra. The results of this work indicate that invariably there is ambiguity in the interpretation of the spectra of small carbide particles. Only in a very few cases can the various phases be conclusively distinguished on the basis of the Mössbauer spectra and parameters currently available in the literature. It will also be shown that if spectra are collected for a single sample over a range of temperatures and if relaxation effects are properly accounted for, the Mössbauer results *can give* not only an accurate identification of the iron phase(s) present but also quantitative particle size information and qualitative information regarding particle structure and the nature of the particle/support interaction.

## EXPERIMENTAL/THEORETICAL

In this study, a Mössbauer modeling routine, described in earlier work (*19–22*), was used to generate theoretical "data" based on bulk phase input parameters, which could then be analyzed using a conventional Mössbauer fitting routine (*23*). The particular phenomena which the model accounts for are (a) superparamagnetic relaxation, as proposed by Wickmann (*24*), (b) collective magnetic excitations, as proposed by Mørup and co-workers (*25*, *26*), (c) log–normal particle distribution (*27*), and (d) changes in the value and distribution of quadrupole splittings due to relaxation and support effects (*22*, *28–30*). In all cases the data input into the modeling routine were those of bulk, nonrelaxed $\chi$-carbide, as reported by Lin and Phillips (*22*). Other information necessary to generate a spectrum included a value of the anisotropy energy constant (*31*), a system temperature, and a value of the quadrupole splitting of the $\chi$-carbide above the Curie temperature (*22*). More thorough descriptions of the modeling program are available elsewhere (*21, 31*). The basis for determining quadrupole splittings as a function of the relaxation time is also discussed elsewhere in the literature (*22*). However, further clarification of this phenomenon is justified and is given below.

*Quadrupole shift distribution.* For compounds which exhibit both an electric field gradient (EFG) at the nucleus and a magnetic hyperfine field (HF), the quadrupole splitting is a function of the angle $\Theta$ between the EFG and the magnetic quadrupole moment of the nucleus. The relationship is given by

$$\Delta E_Q = \tfrac{1}{8}e^2qQ(3\cos^2\Theta - 1), \qquad (1)$$

where $q$ is the EFG and $Q$ is the quadrupole moment. Experimental measurements of unsupported carbide particles exhibit no observable quadrupole splitting. This suggests that the angle $\Theta$ is at the "magic angle" of 54°44′. Other workers have suggested that this is consistent with the crystal structure of the carbide (*32, 33*). However, experiments have also shown that superparamagnetic carbide particles relax to a doublet in the Mössbauer spectrum (*16, 22, 32*). To account for this behavior, Lin and Phillips (*22*) proposed that the following equation be used to model the observed changes in $\Delta E_Q$ for the $\chi$-carbide system:

$$\Delta E_Q = \varepsilon_{\text{curie}}\exp(-\tau/\tau_0), \qquad (2)$$

where $\varepsilon_{\text{curie}}$ is the value of $\Delta E_Q$ observed above the Curie temperature and $\tau_0$ is the value of the relaxation time at the "blocking temperature," defined as the temperature where the magnetically split lines (particularly lines 1 and 6) disappear. For the $\chi$-carbide system $\tau_0$ is approximately $3.8 \times 10^{-9}$ s. This function meets certain clear requirements. First, in the limit of large relaxation times (large particles, low temperature, $\tau \gg \tau_0$), $\Delta E_Q = 0$, as observed. In the other extreme (small particles, high temperature, $\tau \ll \tau_0$), $\Delta E_Q = \varepsilon_{\text{curie}}$, again as observed. In the transition region ($\tau \sim \tau_0$) the spectrum exhibits sharp changes in $\Delta E_Q$ when superparamagnetism becomes important, which can be modeled well by the exponential function. It should be noted here that other functional forms were tested (e.g., linear, quadratic) which produced qualitatively similar spectra.

As a variation of the above equation, Lin and Phillips further proposed that for systems which exhibit a distribution of quadrupole splittings the following be used:

$$\Delta E_Q = \varepsilon_{\text{curie}}\exp(-\tau/\tau_0) + \varepsilon_0(1 - \exp(-\tau/\tau_0)), \qquad (3)$$

where the first term is identical to the original equation and the second accounts for the observed variation of splittings. Here $\varepsilon_0$ is an empirical constant that is varied by small increments between two limits. In the case of large relaxation times, $\tau \gg \tau_0$, the first term vanishes while the second can give a distribution of $\Delta E_Q$ between the limits of $\varepsilon_0$. In the other extreme, $\tau \ll \tau_0$, $\Delta E_Q$ reduces to $\varepsilon_{\text{curie}}$ of the relaxed particles.

The distribution arises from variations of the angle $\Theta$ between the EFG and the magnetic moment of different particles. Such deviations from the magic angle (54°44′) could be expected in systems where crystal growth is affected by interaction with the support. Support interactions change the equilibrium particle shape and this in turn affects the angle between the magnetic easy direction and the EFG. These effects produce broadness of the observed Mössbauer lines that are not seen in unsupported particles or those on weakly interacting supports (*22*). Such an idea can explain the experimental observations. It should be stressed that Eqs. (2) and (3) are empirical equations and that the justification given above is best regarded as a plausibility argument.

TABLE 1

Comparison of Input and Fitted Mössbauer Parameters for a Bulk $\chi$-Carbide Phase[a]

| Parameter | Fe site | Input values | Fitted values |
|---|---|---|---|
| $H_{hf}$ (kOe) | I | 196.0 | 196.5 |
| | II | 217.0 | 217.5 |
| | III | 118.0 | 117.5 |
| $\delta_{IS}$ (mm/s) | I | +0.15 | +0.15 |
| | II | +0.17 | +0.17 |
| | III | +0.15 | +0.14 |
| $\Delta E_Q$ (mm/s) | I | 0.00 | −0.003 |
| | II | +0.027 | +0.025 |
| | III | −0.012 | +0.021 |
| Relative intensity | I | 3:2:1 | 3.9:3.2:1.2 |
| | II | 3:2:1 | 4.0:2.1:1.7 |
| | III | 1.5:1.0:0.5 | 2.0:1.4:0.4 |
| Linewidths (mm/s) | I | 0.25:0.23:0.23 | 0.5:0.43:0.35 |
| | | 0.25:0.23:0.23 | 0.48:0.48:0.46 |
| | III | 0.25:0.23:0.23 | 0.61:0.68:0.79 |

[a] Additional input parameters: (i) anisotropy energy constant = $1 \times 10^6$ erg/cm$^3$; (ii) average particle size = 200 Å; (iii) temperature = 300 K; (iv) $\sigma$ = 1.20.

As stated previously, in all cases studied the starting parameters used were those of bulk $\chi$-carbide as taken from experimental measurements (see Table 1). The data of $\chi$-carbide are the most reliable available for a metastable carbide phase in the composition range of interest at various temperatures. The goals of the work were threefold: (i) to test the accuracy of the model against the standard fitting procedure, (ii) to examine the relaxation behavior of the "known" carbide phase for comparison with the "unknown" ($\varepsilon$, $\varepsilon'$) carbides, and (iii) to see if "$\varepsilon$-like" spectra could be generated via relaxation of the $\chi$-carbide spectrum.

## RESULTS AND DISCUSSION

The reliability of the methodology was first demonstrated in the following manner. A model spectrum of a $\chi$-carbide sample was generated, making sure that all particle sizes in the distribution were large enough to act as bulk material ($\tau \gg \tau_0$ for all particles), which eliminated all relaxation effects. These "data" were then analyzed using the conventional least-squares fitting routine (*23*). Agreement between the input parameters and the fit was excellent (Table 1). One word of explanation of the fitting procedure is warranted at this point. Many workers have found it difficult to obtain good fits to complex spectra of this type. They have usually resorted to constraints on the fitting parameters (i.e., linewidth, line position, relative intensity, splitting ratios) to eliminate anomalous results. In the present work the fitted spectra were constrained only such that the dip and width of corresponding peaks of a sextuplet (1-6, 2-

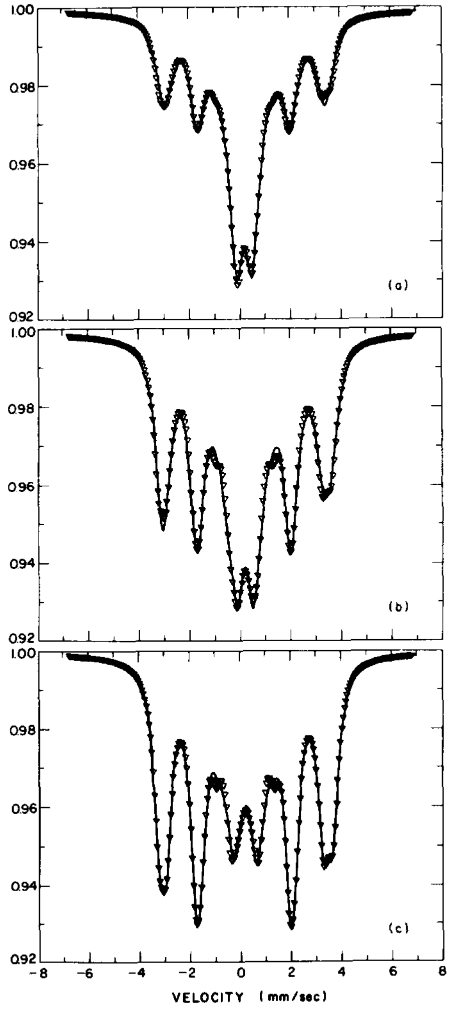

FIG. 1. Effect of anisotropy energy constant on spectrum. (a) $K$ = 750,000 erg/cm$^3$; (b) $K$ = 1,500,000 erg/cm$^3$; (c) $K$ = 3,000,000 erg/cm$^3$. Other input parameters were (i) average particle size = 55 Å; (ii) $\sigma$ = 1.20; (iii) $T$ = 300 K. (Triangles represent generated data.)

TABLE 2

Mössbauer Parameters Obtained from a 20-Peak Fit of the Spectra in Fig. 1

| Spectrum | Spectral component | $H_{\mathrm{hf}}$ (kOe) | $\delta_{\mathrm{IS}}$ (mm/s) | $\Delta E_Q$ (mm/s) | Linewidths (mm/s) | % Area |
|---|---|---|---|---|---|---|
| 1a | χ-I | 192.3 | 0.146 | 0.020 | 0.57 : 0.62 : 0.67 | 24.7 |
| | χ-II | 215.4 | 0.233 | 0.016 | 0.78 : 0.77 : 0.62 | 24.0 |
| | χ-III | 106.7 | 0.241 | −0.027 | 0.61 : 0.62 : 0.61 | 10.3 |
| | Doublet | — | 0.157 | 0.590 | 0.76 | 41.0 |
| 1b | χ-I | 192.6 | 0.140 | 0.009 | 0.61 : 0.50 : 1.4 | 35.3 |
| | χ-II | 212.3 | 0.178 | 0.023 | 0.55 : 0.55 : 0.44 | 28.6 |
| | χ-III | 110.3 | 0.183 | −0.019 | 0.72 : 0.88 : 0.51 | 20.1 |
| | Doublet | — | 0.152 | 0.533 | 0.60 | 16.0 |
| 1c | χ-I | 192.0 | 0.146 | −0.002 | 0.49 : 0.69 : 0.62 | 36.6 |
| | χ-II | 212.4 | 0.165 | 0.027 | 0.57 : 0.53 : 1.0 | 38.8 |
| | χ-III | 113.9 | 0.162 | −0.020 | 0.52 : 0.64 : 0.63 | 19.8 |
| | Doublet | — | 0.181 | 0.879 | 0.75 | 4.8 |

5, 3-4) were equal. Good fits could usually be obtained using only this assumption.

A series of model spectra were produced to systematically test the effect of a variation of the input parameters on the observed spectra. In Fig. 1 the results of a variation of the anisotropy energy constant are shown. All other parameters were held constant; their values are listed in the figure caption. It is obvious that variation of this parameter has a significant impact on the appearance on the spectra. The results of fitting the model data are given in Tables 2 and 3. In most cases good fits could be obtained assuming only a single sextuplet and a superparamagnetic doublet were present (see solid curves shown in Fig. 1). The decision to fit the spectra as a single sextuplet and a doublet was based on a visual inspection of the data. That is, the fitting was done as if the data represented an unknown phase of iron. This is the same rationale used by Amelse (*7*) for fitting the data of ε′-carbide. Addition of more sextuplets did not visually improve the fit but were necessary to confine the intensity ratios of the sextuplet peaks to the desired 3 : 2 : 1.

The effect of relaxation can be clearly

TABLE 3

Mössbauer Parameters Obtained from an 8-Peak Fit of the Spectra in Figs. 1 and 2

| Spectrum | Spectral component | $H_{\mathrm{hf}}$ (kOe) | $\delta_{\mathrm{IS}}$ (mm/s) | $\Delta E_Q$ (mm/s) | Linewidths (mm/s) | % Area |
|---|---|---|---|---|---|---|
| 1a | Sextuplet | 197.7 | 0.155 | 0.014 | 0.77 : 0.70 : 1.6 | 58.4 |
| | Doublet | — | 0.158 | 0.643 | 0.73 | 41.6 |
| 1b | Sextuplet | 200.4 | 0.155 | 0.013 | 0.75 : 0.61 : 1.7 | 73.8 |
| | Doublet | — | 0.159 | 0.748 | 0.79 | 26.2 |
| 1c | Sextuplet | 202.0 | 0.154 | 0.013 | 0.74 : 0.59 : 1.0 | 92.8 |
| | Doublet | — | 0.210 | 1.209 | 1.40 | 7.2 |
| 2a | Sextuplet | 199.4 | 0.155 | 0.013 | 0.75 : 0.69 : 1.19 | 55.0 |
| | Doublet | — | 0.160 | 0.681 | 0.73 | 45.2 |
| 2b | Sextuplet | 197.6 | 0.155 | 0.014 | 0.78 : 0.61 : 1.02 | 79.2 |
| | Doublet | — | 0.165 | 1.594 | 2.12 | 20.8 |
| 2c | Sextuplet | 198.2 | 0.157 | 0.013 | 0.73 : 0.55 : 0.54 | 91.4 |
| | Doublet | — | 0.182 | 2.300 | 0.692 | 8.6 |

seen on the values of the hyperfine fields. In the 20-peak fits (Table 3), all three values of the hyperfine splitting are lower than the fit of the bulk (Table 1) values. In the case of the 8-peak fits, the hyperfine field represents an average of sorts. Also, it can be seen that as relaxation becomes more important, the lines tend to broaden somewhat and the fits become more difficult. Furthermore, there is very little improvement in the overall fit if 20 instead of 8 lines are assumed. Indeed, even sensitive parameters such as linewidth are not greatly closer to the input parameters if 20 lines instead of 8 are used to fit the data. Thus, choosing to fit a relaxed spectrum with three sextuplets instead of a single sextuplet can only be justified in cases in which it is known by other means that a particular carbide is present. In other words, a relaxed spectrum represents a "flexible" fit in which the initial assumptions strongly influence the result.

One other observation can be made. Even for an anisotropy energy constant of 3 × $10^6$ erg/cm$^3$, some relaxation is observed for the chosen distribution of particles (average radius = 55 Å). Other work, not shown, indicates that for smaller (35-Å radius) particles, a relaxed doublet will dominate the spectrum even for anisotropy energy constants as high as 5 × $10^6$ erg/cm$^3$. When the anisotropy energy constant is raised to 1 × $10^7$ erg/cm$^3$, the hyperfine splitting can again be observed, but noticeable relaxation effects are still present. Such large values of this parameter have only been reported in a few noniron systems with hexagonal symmetry (*31*). The contribution to the anisotropy energy constant from crystalline anisotropy is an order of magnitude larger for hexagonal crystals than cubic crystals. The high carbon content of the octahedral carbides might lead to considerable lengthening of the *c*-axis of the hexagonal crystal (*1*, *15*), causing a larger crystalline anisotropy. This could explain this unusually high value of the anisotropy energy constant. However, there is an

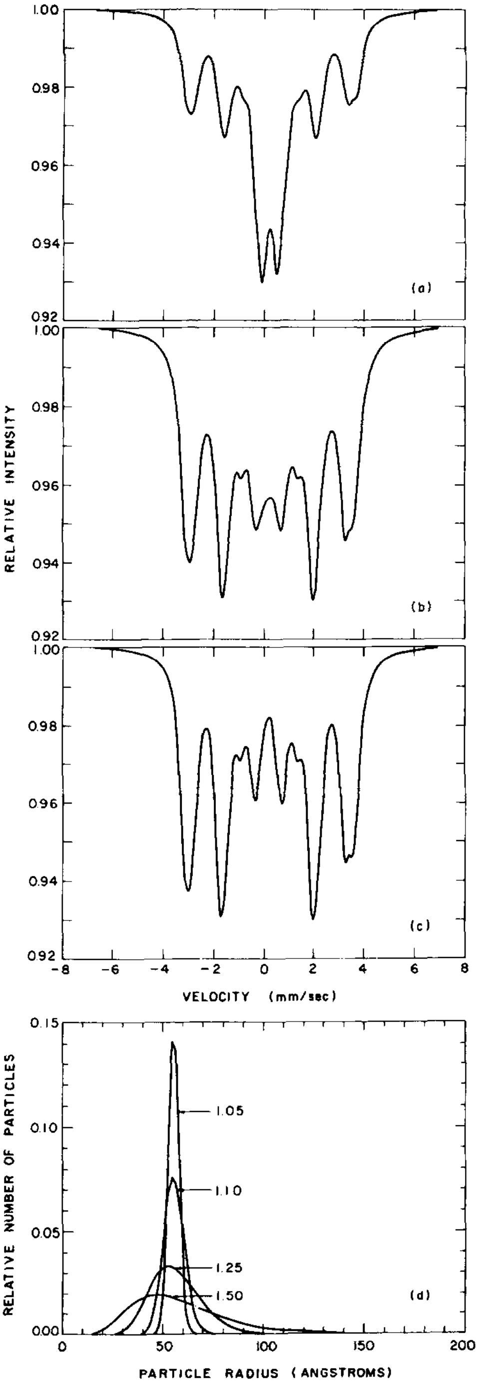

FIG. 2. Effect of narrowness of particle size distribution on spectrum. (a) $\sigma$ = 1.25; (b) $\sigma$ = 1.10; (c) $\sigma$ = 1.05; (d) log–normal distribution function for several $\sigma$ values. Other input parameters were (i) average particle size = 55 Å; (ii) $T$ = 300 K; (iii) anisotropy energy constant = 1,000,000 erg/cm$^3$.

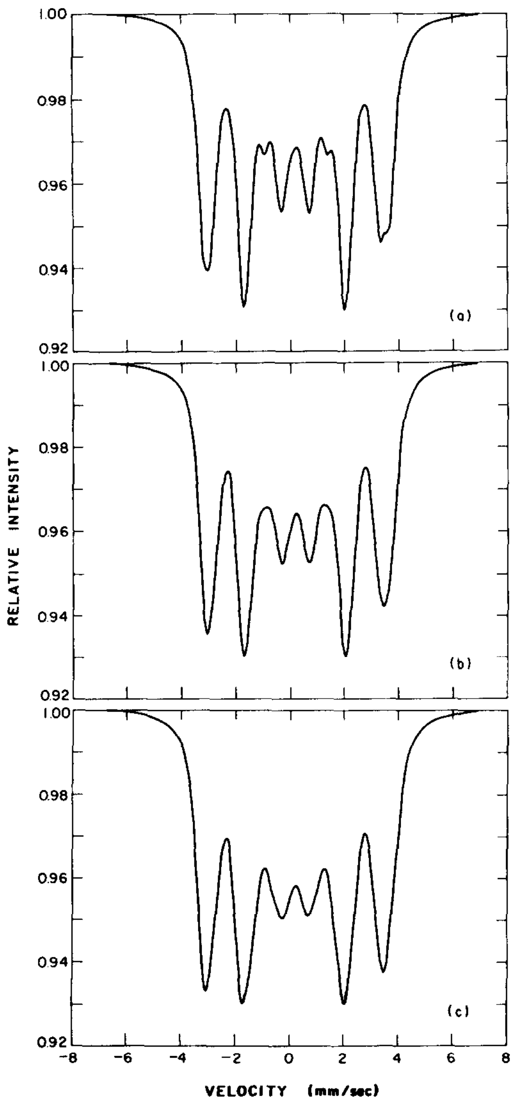

FIG. 3. Effect of a variation of $\varepsilon_0$ (Eq. (3), Ref. (*22*)). (a) $\varepsilon_0 = 0$; (b) $-0.5\varepsilon_{\text{curie}} < \varepsilon_0 < 0.5\varepsilon_{\text{curie}}$; (c) $-0.75\varepsilon_{\text{curie}} < \varepsilon_0 < 0.75\varepsilon_{\text{curie}}$. Other input parameters were (i) average particle size = 80 Å; (ii) $\sigma = 1.20$; (iii) $T = 300$ K; (iv) anisotropy energy constant = 1,000,000.

alternate explanation. A value of the anisotropy energy constant greater than $1 \times 10^7$ erg/cm$^3$ is so much larger than any previously reported for any iron system that it seems physically unreasonable. Thus reports of $\varepsilon$- and $\varepsilon'$-carbide particles of average radius as small as 35 Å, which produce only partially relaxed spectra, are suspect. Additional investigation is warranted.

Figure 2 demonstrates the impact of variation in the value of $\sigma$, the nondimensional geometric standard deviation of the log-normal particle distribution function (*27*). The shape of the resultant distributions is shown in Fig. 2d for various values of $\sigma$. As can be seen, the distribution approaches that of a spike at the average particle size as $\sigma$ approaches 1.0. Again, there is a startling effect of this parameter on the observed spectra. One point that can be made is that, in this case, there is not a significant line broadening seen as the distribution widens (Table 3). This would indicate that the broadness of lines seen in the spectra of $\varepsilon'$-carbide may not be solely attributable to a wide particle size distribution as has been proposed (*5–7*). Clearly, some other phenomenon is responsible for the observed line broadening.

In Fig. 3, variations in the quadrupole splittings were introduced. This was done by varying the value of $\varepsilon_0$ slightly between two limits (listed in Fig. 3). This not only causes the lines to broaden significantly but also has a profound effect on the appearance of the entire spectrum. In previous work (*22*) it was shown that a variation in the value of the quadrupole distribution could explain many unusual spectral features. As was argued earlier, it is reasonable to assume that such a distribution would be seen for a particle on an amorphous or strongly interacting support. Here, it can be seen that the effect of the broadening is the removal of much of the detail from the spectrum, resulting in something that gives the appearance of a single asymmetric sextuplet with broad lines. The classic $\varepsilon'$-carbide spectrum is similar in appearance (*7*).

Several workers have suggested that $\varepsilon'$-carbide has the stoichiometry, $Fe_{2.2}C$. However, there is no crystal structure that can be rationalized to support the $Fe_{2.2}C$ stoichiometry and still provide a unique Fe atom environment. LeCaër *et al.* (*1*) suggested that the octahedral carbides exist as a hexagonal array of iron atoms with the

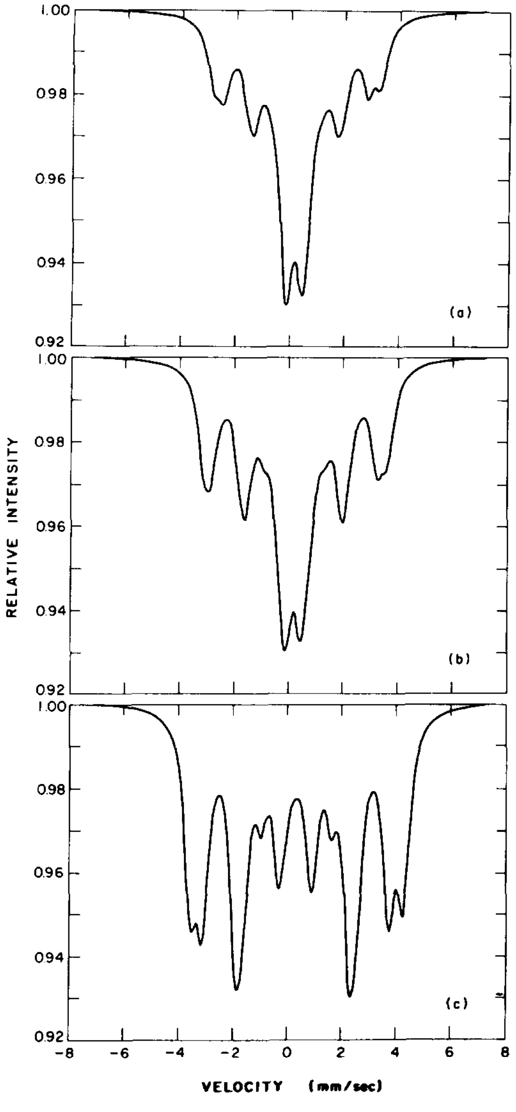

Fig. 4. Effect of temperature on spectrum. (a) $T$ = 350 K; (b) $T$ = 300 K; (c) $T$ = 80 K. Other parameters were (i) average particle size = 55 Å; (ii) $\sigma$ = 1.20; (iii) anisotropy energy constant = 1,000,000 erg/cm$^3$. Values of $H_{\mathrm{hf}}$ and $\delta_{\mathrm{IS}}$ were taken from Ref. (*22*) at each temperature.

carbon atoms "statistically" distributed in the octahedral interstices. There is a range of carbon contents that would be accommodated by such an arrangement, from approximately $Fe_{2.4}C$ to $Fe_2C$. Such an atomic arrangement could have an effect similar to that produced in Fig. 3. Each Fe atom would exist in a slightly different environment leading to a distribution of hyperfine fields and quadrupole splittings around the average value(s). It is reasonable to assume that a Mössbauer spectrum of such a system would appear as a broad and possibly asymmetric sextuplet.

Other parameters which were varied in this study included average particle size and temperature. Changes in these parameters produced significant but predictable changes in the spectra as seen in Fig. 4 and elsewhere (*22*). Finally, an attempt was made to take advantage of the contribution of collective magnetic excitations (*25, 26*) to the relaxation process. It was hoped that, at particle sizes of <35 Å radius, the hyperfine field of the $\chi$-carbide system would be reduced to 85% of its bulk value, or 170 kOe, the reported field of $\varepsilon'$-carbide. However, extensive work showed that it was not possible to achieve this 15% reduction without introducing an overwhelming superparamagnetic doublet to the spectrum. Hence, the reported 170-kOe field cannot be attributed to a relaxed $\chi$-carbide spectrum.

## CONCLUSIONS

Some conclusions regarding the current state of knowledge of the phases of carbide formed during Fischer–Tropsch synthesis can be drawn from a careful consideration of the model data presented here and a critical evaluation of published spectra.

First, there is ample evidence to support the conclusion that at least one phase of octahedral carbide, normally called $\varepsilon'$ carbide, forms during Fischer–Tropsch synthesis and that a partially relaxed spectrum of this phase can be well represented by a single sextuplet with the following average parameters: isomer shift (IS) = 0.25 mm/s, hyperfine field = 170 kOe (*1, 12*). However, on the basis of the reported particle sizes (obtained via X-ray line broadening the chemisorption), the clear asymmetry of the $\varepsilon'$ spectra, and the lack of a unique Fe atom environment in the assumed $\varepsilon'$-carbide crystal, it is reasonable to suggest that the spectra of $\varepsilon'$-carbide probably consists of at least two sextuplets. The value of the unrelaxed hyperfine fields at room temperature are not accurately known but are almost certainly larger than 170 kOe. As in the case of partially relaxed $\chi$-carbide, the 170-kOe field probably represents an average of the relaxed multiple sextuplets. In addition the broadness of the lines could be attributed to (i) the variation of Fe atom environments that would be present in a hexagonal phase with a statistical distribution of carbon atoms in octahedral holes, (ii) the superposition of the multiple sextuplets that probably exist, and/or (iii) the effects of relaxation on the linewidth. On the basis of the work presented, however, it should be clear that the broadness cannot be solely explained by assuming a wide particle distribution.

The second metastable phase ($\varepsilon$-carbide), generally associated with a high field sextuplet ($H_{\mathrm{hf}}$ = 240 kOe), has never been reported as more than small background lines, not large enough to obtain reliable quantitative information. It is equally likely that this second sextuplet is a contribution from a small amount of partially related $\chi$-carbide present in the sample. This possibility has been discussed by others (*1, 3, 6*). Indeed, similar arguments have been used to discount the contribution to the spectrum of a sextuplet with a hyperfine field of 130 kOe (*1*). In summary, there are insufficient Mössbauer data to support the contention that $\varepsilon$-carbide exists as a distinct octahedral carbide phase.

It should be clear that without careful evaluation of all parameters contributing to the Mössbauer spectrum of the carbide phases, good quantitative information is difficult, if not impossible, to obtain. Also, this work indicates that reliable Mössbauer parameters and phase identifications are only possible for phases which represent a significant fraction of the total spectral area, and only when relaxation effects are properly accounted for. If relaxation effects become important then spectra should be collected over a wide range of temperatures and modeling routines employed to aid in the identification of the phase or phases present in the sample.

## REFERENCES

*1.* LeCaër, G., Dubois, J. M., Pijolat, M., Perrichon, V., and Bussiere, P., *J. Phys. Chem.* **86,** 4799 (1982).
*2.* Jung, H.-J., Vannice, M. A., Mulay, L. N., Stanfield, R. M., and Delgass, W. N., *J. Catal.* **76,** 208 (1982).
*3.* Tau, L. M., Borcar, S., Bianchi, D., and Bennett, C. O., *J. Catal.* **87,** 36 (1984).
*4.* Bianchi, D., Borcar, S., Teule-Gay, F., and Bennett, C. O., *J. Catal.* **82,** 442 (1983).
*5.* Raupp, G. B., and Delgass, W. N., *J. Catal.* **58,** 337,348 (1979).
*6.* Niemantsverdriet, J. W., van der Kraan, A. M., van Dijk, W. L., and van der Baan, H. S., *J. Phys. Chem.* **84,** 3363 (1980).
*7.* Amelse, J. A., Butt, J. B., and Schwartz, L. H., *J. Phys. Chem.* **82,** 558 (1978).
*8.* Maksimov, Yu. V., Suzdalev, I. P., Arents, R. A., Goncharov, J. V., Krautsov, A. V., and Loktev, S. M., *Kinet. Katal.* **13**(6), 1600 (1972).
*9.* Maksimov, Yu. V., Suzdalev, I. P., Arents, R. A., and Loktev, S. M., *Kinet. Katal.* **15**(5), 1293 (1974).
*10.* Loktev, S. M., Makarenkova, L. I., Slivinskii, E. V., and Entin, S. D., *Kinet. Katal.* **13**(4), 1042 (1972).
*11.* Arents, R. A., Maksimov, Yu. V., Suzdalev, J. P., Imshennik, V. K. and Krupyanskiy, Yu. F., *Fiz. Met. Metalloved.* **36**(2), 277 (1973).
*12.* Ron, M., *in* "Applications of Mössbauer Spectroscopy" (R. L. Cohen, Ed.), Vol. II, p. 329, Academic Press, New York, 1982.
*13.* Mathalone, Z., Ron, M., Pipman, J., and Niedzwiedz, S., *J. Appl. Phys.* **42**(2), 687 (1971).
*14.* LeCaër, G., Simon, A., Lorenzo, A., and Genin, J. M., *Phys. Status Solidi A* **6,** K97 (1971).
*15.* Bernas, H., Campbell, J. A., and Fruchart, R., *J. Phys. Chem. Solids* **28,** 17 (1967).
*16.* LeCaër, G., Dubois, J. M., and Senateur, J. P., *J. Solid State Chem.* **19,** 19 (1976).
*17.* Hofer, L. J. E., Cohn, E. M., and Peebles, W. C., *J. Amer. Chem. Soc.* **71,** 189 (1949).
*18.* Barton, G. H., and Gale, B., Acta Crystallogr. **17,** 1460 (1964).
*19.* Phillips, J., Clausen, B., and Dumesic, J. A., *J. Phys. Chem.* **81,** 1814 (1980).
*20.* Phillips, J., and Dumesic, J. A., *Appl. Surf. Sci.* **7,** 215 (1981).
*21.* Phillips, J., Chen, Y., and Dumesic, J. A., *in* "New Surface Science in Catalysis" (M. L. Deviney and J. Gland, Eds.) *ACS Symposium Series,* p. 518 (1985).

22. Lin, S.-C., and Phillips, J., *J. Appl. Phys.* **58**(5), 1943 (1985).
23. Sørensen, K., "International Report No. 1, Laboratory of Applied Physics II (Technical University of Denver, 1972).
24. Wickmann, H. H., *in* "Mössbauer Effect Methodology" (I. J. Gruverman, Ed.), Vol. 2, p. 39. Plenum, New York, 1966.
25. Mørup, S., and Topsøe, H., *Appl. Phys.* **11,** 63 (1976).
26. Mørup, S., Topsøe, H., and Lipka, J., *J. Phys. (Paris) Colloq.* **37,** C6-287 (1978).
27. Granqvist, C. G., and Buhrman, R. A., *J. Catal.* **42,** 477 (1976).
28. Blume, M., and Tjon, T. A., *Phys. Rev.* **165,** 447 (1968).
29. Blume, M., *Phys. Rev. Lett.* **18,** 305 (1967).
30. Bradford, E., and Marshall, W., *Proc. Phys. Soc. London* **87,** 731 (1966).
31. Mørup, S., Dumesic, J. A., and Topsøe, H., *in* "Applications of Mössbauer Spectroscopy" (R. L. Cohen, Ed.), Vol. II, p. 1 Academic Press, New York 1980.
32. Maksimov, Yu, V., Suzdalev, I. P., and Arents, R. A., *Sov. Phys. Solid State* **14,** 2832 (1973).
33. Ron, M., and Mathalone, Z., *Phys. Rev. B* **4,** 774 (1971).